Cerebral Cortex, 2026, 36, bhag176
https://doi.org/10.1093/cercor/bhag176
Published: 26 October 2026
Original Article

OXFORD

Cortical folding and reduced connection distances in the human brain

Edmund T. Rolls [1,2,3,*], Yichun Huang [4] and Chu-Chung Huang [5,*]

[1]Oxford Centre for Computational Neuroscience, Oxford, United Kingdom
[2]Department of Computer Science, University of Warwick, Coventry CV4 7AL, United Kingdom
[3]Institute for the Science and Technology of Brain-Inspired Intelligence, Fudan University, Zhangjiang High Tech Park, Shanghai 201203, China
[4]School of Psychological and Cognitive Sciences; Beijing Key Laboratory of Behavior and Mental Health; IDG/McGovern Institute for Brain Research; Peking-Tsinghua Center for Life Sciences, Peking University, Beijing 100871, China
[5]Shanghai Key Laboratory of Brain Functional Genomics (Ministry of Education), Institute of Brain and Education Innovation, School of Psychology and Cognitive Science, East China Normal University, Shanghai 200602, China

*Corresponding authors: Edmund T. Rolls, Department of Computer Science, University of Warwick, Coventry CV4 7AL, United Kingdom. Email: Edmund.Rolls@oxcns.org; Chu-Chung Huang, School of Psychology and Cognitive Science, East China Normal University, Shanghai 200602, China. Email: czhuang@psy.ecnu.edu.cn

Why do sulci occur in the human brain in particular parts of the cortical sheet? To obtain quantitative evidence on how folding may help to reduce the amount of white matter involved in connecting cortical regions, we measured the geodesic distance (GD) across the cortical white-matter surface, and the length of the connections and the number of streamlines (SN), between 180 cortical regions in the Human Connectome Project (HCP) Multimodal Parcellation atlas using diffusion tractography at 7 T in 178 HCP participants. For relatively long connections (GD >90 mm), we quantify how in many cases the connection distance is much shorter than the geodesic distance, with the presence of folding making this possible. We show how sulci can help to reduce the wiring cost defined as the length of the streamlines multiplied by the number of streamlines between all cortical regions. The wiring cost function may be minimized in evolution by utilizing factors such as the "tension" between cortical regions caused by the number of streamlines and the distance that could be saved arising from having sulci in particular locations in the cortical sheet. The cortical folding may also bring key hierarchically organized cortical processing streams closer together to minimize conduction time.

Keywords brain size, cerebral cortex, cortical folding, diffusion tractography, geodesic distance, sulci

Introduction

The human cerebral cortex is highly convoluted, with many fissures and sulci. This provides for a large cortical area but a relatively low brain volume. But the question arises about why the sulci are where they are. There has been much interest in the many factors that may influence cortical folding during the development of the brain (Van Essen 2023). One example is differential migration of cells to superficial vs deep layers of the developing cortex, which may produce cortical folding (Van Essen 2023). Another factor may be differential expansion of outer and inner zones of the cortical sheet during development due to their different biomechanical properties (Herculano-Houzel et al. 2010; Xu et al. 2010; Bayly et al. 2014; Fernandez et al. 2016; Kroenke and Bayly 2018; Llinares-Benadero and Borrell 2019; Fernandez and Borrell 2023). Another factor that may influence cortical folding is tension between connections connecting regions during cortical development (Van Essen 1997; Herculano-Houzel et al. 2010; Van Essen et al. 2019; Van Essen 2020, 2023). In more detail, the axon tension hypothesis is that cortical regions with many connections between them might be pulled together during brain development by the tension in the axons, to form for example a gyral crown (Van Essen 1997; Van Essen et al. 2019; Van Essen 2020, 2023). An important function of the tension between developing cortical regions caused by the white matter connections could be to help reduce the connection distances (CDs) between highly connected cortical regions to reduce brain weight and volume (Van Essen 2023). Minimizing brain weight is likely to be important in land animals for locomotion, especially in species that walk upright on 2 legs such as humans (Rolls 2023a, 2026a). Minimizing brain volume is likely to be important also in mammalian childbirth, especially in humans with a bipedal posture with its implications for the pelvic regions which results in humans being born with relatively immature brains (Rolls 2023a, 2026a). Even the self-organization of topological maps in the cerebral cortex may have the important function of minimizing the CDs between neurons that are involved in the same computation (Rolls 2016, 2023a, 2026a, 2026b).

However, no quantitative analysis or theory of why the sulci are where they are in the human brain is available, as far as we know. The aim of the research described here is to investigate how in the human brain the locations of the sulci may contribute to reducing the CDs between cortical areas with many connections between them, which may help to keep human brain weight and volume relatively low.

Received: April 23, 2026. **Revised:** September 7, 2026. **Accepted:** September 29, 2026
© The Author(s) 2026. Published by Oxford University Press. All rights reserved. For commercial re-use, please contact reprints@oup.com for reprints and translation rights for reprints. All other permissions can be obtained through our RightsLink service via the Permissions link on the article page on our site—for further information please contact journals.permissions@oup.com.

Downloaded from academic.oup.com/cercor/article/36/10/bhag176/9002283 by guest on 27 October 2026

In the research described here, we investigate why the sulci and fissures are where they are in the human brain, and in particular how the location of sulci may help to reduce the amount of white matter that connects different cortical regions. We recognize that any influence of relatively small CDs between highly connected cortical areas may reflect processes that apply at different stages of brain development. We measure the geodesic distance (GD) between cortical regions along the surface defining the boundary between cortex and white matter, and the CD between the same cortical regions using diffusion tractography, and the number of streamlines (SN) in each connection between the cortical regions. We find which CDs are shorter than the GD, and show that in some clear cases the shorter CD is provided for by folding. One example is that the insula regions deep in the Sylvian or lateral fissure benefit by having a relatively short CD to some premotor area 6 regions, and that provides an advantage of the lateral or Sylvian fissure. But we then go on to quantify the savings provided by each direct connection by computing the reduction in the CD compared to the GD multiplied by the SN in that connection. This leads to a hypothesis that the places where cortical folding preferentially gives rise to sulci can be accounted for at least in part by the savings in the total connection length (distance saved multiplied by the number streamlines or fibers) between cortical regions.

The Human Connectome Project Multimodal Parcellation (HCP-MMP) was used for this investigation, because it includes a surface map of the cortex with a large number, 180 per hemisphere, of cortical regions carefully defined based on anatomy (cortical thickness and myelin), functional connectivity, and on task-related functional magnetic resonance imaging (fMRI) (Glasser et al. 2016). By measuring GDs across the cortical sheet at the base of the cortex, and measuring CD via fiber tracking with diffusion tractography, we were able to quantify the geometric and connectivity relationships between cortical regions, thereby providing evidence to help elucidate hypotheses regarding cortical folding principles. This is the first quantitative attempt to perform this type of detailed analysis for the human brain, as far as we know.

Methods

Dataset and participants

Data from 178 participants (69 males and 109 females, aged 22 to 36 yrs) were included from the publicly available Wu-Minn HCP 7 T dataset. All individuals had completed both diffusion-weighted (dMRI) and structural (T1-weighted, T1w) MRI scans. Preprocessed dMRI and T1w images were obtained from the ConnectomeDB platform (https://db.humanconnectome.org). Briefly, T1w images were processed following the HCP minimal preprocessing pipelines, including tissue segmentation and cortical surface reconstruction using FreeSurfer. The resulting inner white matter and outer pial surfaces were subsequently registered to the standard fs_LR 32 k surface template. To determine the location of the main sulci, sulcal depth data were obtained from the HCP S1200 group average data. The dMRI images were preprocessed based on the updated diffusion pipeline (v3.19.0), as described by Glasser et al. (2013).

Flattened map of the human cerebral cortex

Figure 1 (lower) shows a flattened map of the HCP Parcellation (HCP-MMP) of the human brain (Glasser et al. 2016), to provide an idea of the distances across the surface of the human brain between cortical regions. The GD across the surface at the bottom of the cortex where it joins white matter of the real folded brain was calculated as described next. Figure 1 (upper) shows 3 views of the inflated human brain with the sulci considerably opened to show the different cortical regions. Figure S1-5 shows unfolded images of the human brain with the HCP-MMP parcellation to show how much cortical folding there is. Figure S1-1:4 shows coronal slices through the human brain with the HCP-MMP regions labeled. Figure S1-1:4 helps to visualize how sulci can shorten the CDs through the white matter between some pairs of cortical regions. A list of the cortical regions in the HCP-MMP atlas and their divisions is provided in Table S1.

Geodesic distance

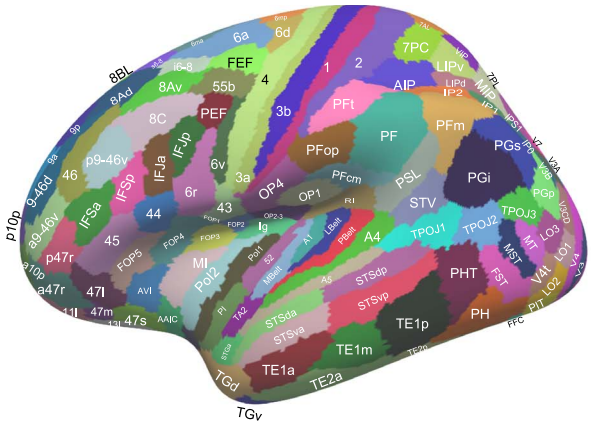
GDs between grayordinate vertices were calculated using the Connectome Workbench software (version 1.5.0) and the Brainsmash Python package (version 0.11.1) with the "cortex" function (https://brainsmash.readthedocs.io/) (Burt et al. 2020). This approach utilizes Dijkstra's algorithm to determine the shortest path between each pair of vertices on a graph. Individual GDs were computed at the white matter surface at the base of the cortex and where direct connections at the base of the cortex could run. We measured the distances at the depth of the cortex, where it adjoins white matter, for then the CD would be little affected even if the cortical sheet was forced into a 3D shape that might approximate a sphere. To illustrate what is meant by the GD, in Fig. 6 in the slice at $y = +10$, the single dashed red line shows what is meant by the GD, and how it can be longer than the actual CD of the streamlines between these cortical regions. The GDs measured in this way thus reflect the distance that fibers would need to travel if they remained close to the lower surface of the cortex even if it was folded. This contrasts with the actual distances that arise when the actual paths of the connections are mapped in the human brain, which can be much shorter because of the presence of sulci, as shown in this research. To ensure that the measured GDs reflect anatomically valid paths not blocked by the interhemispheric juncture, distances were measured on the white matter surface along the anatomical regions visualized in the flattened map in Fig. 1. Following the approach utilized by Lv et al. (2023), we avoided calculating distances directly between the top and bottom edges of the cortical map by setting the "medial" parameter of the brainsmash "cortex" function to the individual's medial wall mask. We emphasize that the GDs were measured as the shortest path that would connect two cortical regions in the real brain at the base of the cortical gray matter, and were not measured in a flattened map as that would introduce distortions.

For each parcel, region-wise GDs were obtained by averaging all pairwise surface-based distances between vertices within the respective parcels. For a long, thin region (eg the superior temporal sulcus), the algorithm considers all vertex pairs across the region's extent, rather than a single centroid. This captures the spatial distribution of distances, making it more robust than centroid-based methods. Finally, the group-level GD matrix was derived by averaging the distances across all participants.

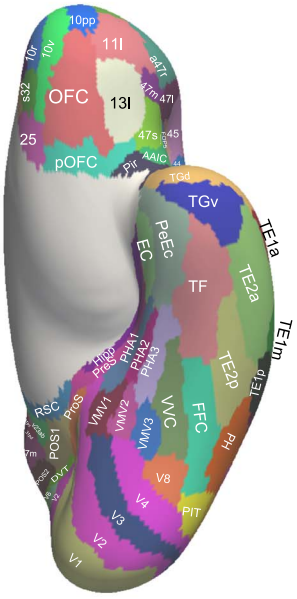
Connection distance and streamline number

A multi-shell multi-tissue constrained spherical deconvolution combined with anatomically constrained tractography was performed to reconstruct fiber orientation distribution (FOD) using the iFOD2

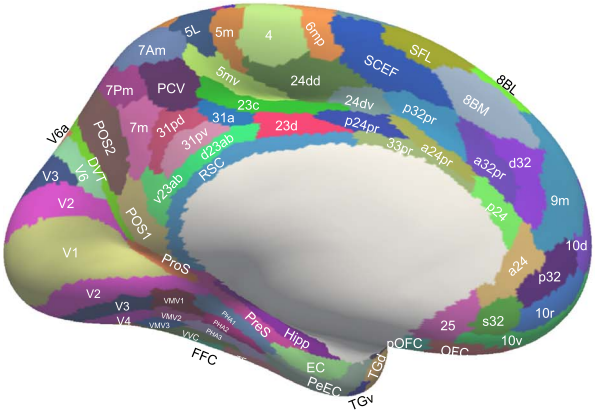
Downloaded from academic.oup.com/cercor/article/36/10/bhag176/9002283 by guest on 27 October 2026



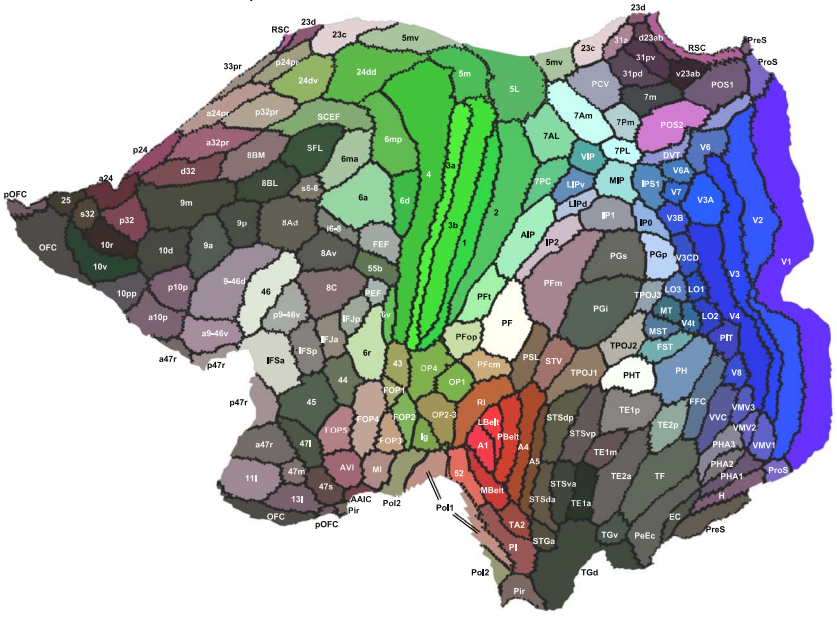
HCP-MMP1 human brain parcellation: lateral view



Inferior view



HCP-MMP1 human brain parcellation: medial view



HCP-MMP1 human brain parcellation: flattened map

Figure 1 Upper 3 images: regions in the HCP-MMP atlas (Glasser et al. 2016) and its extended version HCPex (Huang et al. 2022) to show the cortical regions. The regions are shown on images of the human brain with the sulci expanded sufficiently to allow the regions within the sulci to be shown. Abbreviations are provided in Table S1. For comparison, a version of this diagram without the sulci expanded is provided in Fig. S1-5. The color scheme used is that of HCPex (Huang et al. 2022) which was adopted because it has high color contrast enabling cortical regions to be easily distinguished, and also because HCPex adds subcortical regions that need different colors. Lower image: a flattened map of the HCP-MMP parcellation, to provide an idea of the distances across the surface of the brain between cortical regions. We note that a flattened map inevitably produces distortions, so is used for illustrative purposes only. In the flattened map, the hippocampus abbreviation is H not Hipp. The GDs were not measured on the flattened map, but were measured on the 3D brain. The color scheme used for the flattened map is that provided by the Connectome Workbench (https://www.humanconnectome.org/software/connectome-workbench.)

Downloaded from academic.oup.com/cercor/article/36/10/bhag176/9002283 by guest on 27 October 2026

method. A dynamic seeding algorithm was employed, generating 20 million streamlines (maximum tract length = 250 mm, minimal tract length = 5 mm, FOD amplitude = 0.05, curve angle = 45°) (Tournier et al. 2010; Smith et al. 2015b). Dynamic seeding uses the spherical-deconvolution informed filtering of tractography (SIFT) model to preferentially place seeds in pathways that remain under-represented relative to the fiber density estimated from the FOD image. It improves the distribution of reconstructed streamline density but does not replace SIFT filtering (Smith et al. 2015a). The registered 5tt image was used as prior biological information to ensure that the streamlines terminated at the Gray Matter-White Matter interface (Smith et al. 2012). To improve the estimation of structural connection density and to reduce false-positive streamlines, the SIFT was then applied, resulting in 2 million streamlines per participant (Smith et al. 2013). Because we wished to measure the CD of the streamlines between pairs of cortical regions, the SIFT2 algorithm that we used in our previous work (Huang et al. 2021) was not considered. SIFT2 weights down the streamlines' connection densities rather than eliminating streamlines likely to be false positive based on FOD. Thus, this approach is not applicable in the case when calculating median fiber length; therefore, we used a slightly different method, as in Yu et al. (2025). The correlation between the two methods for the SN was 0.98, showing excellent consistency. Structural connectomes were generated based on the Human Connectome Project extended (HCPex) atlas, which contains 360 cortical regions and 66 subcortical regions. The atlas was transformed into DWI native space. The SN and median streamline length (taken across the streamlines for each region) between each pair of brain regions were measured, producing 426 × 426 matrices for each individual.

Each reconstructed streamline represents a model-generated trajectory and does not correspond 1-to-1 with a biological axon. Accordingly, after SIFT, streamline counts were interpreted as a relative measure that is more consistent with the underlying diffusion-derived fiber density than unfiltered tractograms, rather than as an estimate of the absolute number of connecting axons.

The median value across individual participants of the CD and SN was used in the analyses described here. The dataset consisted of imaging from 178 HCP participants at 7 T, using the HCP-MMP1 surface-based parcellation (Glasser et al. 2016).

We note that the CDs measure direct distances between connected voxels, which are then averaged within a pair of brain regions. In topologically mapped systems, such as the early visual cortical regions with retinotopic mapping, and somatomotor cortical regions with somatic mapping, some of the CDs can be very short, for example at the boundary between V1 and V2. This is in contrast with the GDs, which reflect the mean distance between all voxels within a pair of cortical regions. The consequence is that the CDs can be shorter than the GDs for nearby topologically mapped regions. For that reason, so as not to distort the analyses described here, we focus on the connectivities between distant cortical regions, separated by eg 90 or more mm of GD (ie the GDs were thresholded to include connections with GDs ≥90 mm), where local factors are less important, in order to investigate how at least for large pathways between distant cortical regions, the presence of cortical folding can contribute to less white matter. However, this does enable us to make the useful point that connections between adjacent topologically mapped regions where the topology is reflected at the border, for example at the border between V1 and V2, may make a contribution to minimizing white matter.

Analysis of the relation between CD, GD, the SN, and the saving of connection numbers from relatively short CDs

Matrices for the 180 regions in a hemisphere in the HCP-MMP1 atlas (Glasser et al. 2016) of the GD between all pairs of cortical regions, and the corresponding SN and CDs for the streamlines between the pairs of cortical regions were prepared as described above. Subsequent analyses were only performed for pairs of cortical regions above a noise/low connectivity threshold of 100 streamlines. The sparseness of the resulting matrices (ie the proportion of non-zero entries) was 0.205. The maximum SN was 1.8×10^5. The Geodesic and CDs are in mm.

A ratio of the CD/the GD revealed pairs of cortical regions with this ratio <1.0 that potentially benefited from a sulcus because their direct streamline CD were shorter than their GD.

A measure that we developed showed the link cost saving in white matter, by weighting the difference between the GD and the actual CD (in mm) multiplied by the SN in that connection. That Link Cost Saving measure provides an estimate of the amount of white matter that is saved by having a direct connection, and is important, as we hypothesize that minimizing the amount of white matter is a factor that may influence where sulci form in order to help minimize brain size.

Supplementary analysis with surface-based registration

To determine whether surface-based registration produced materially different connectivity estimates from the conventional volume-based approach used here for the structural connectivity analysis, we performed a subject-specific sensitivity analysis in 169 of the 178 participants in the HCP 7 T cohort for whom the required preprocessed HCP surface data were available. The standard HCP-MMP1 labels were transferred to each participant's native cortical surface through the individual MSMAll surface correspondence (multimodal surface matching based on cortical areal features), projected through the white-pial ribbon into native T1w space, transformed into diffusion space, and combined with the native-space HCPex subcortical labels. This procedure retained the same 426-region atlas organization while allowing us to examine the influence of cortical registration on the resulting connectivity matrices. The surface-derived and volume-derived branches used identical filtered tractograms and endpoint-assignment settings. This supplementary analysis showed that the two parcellation methods produced highly similar group-level streamline-count connectivity matrices ($r = 0.98$). This supplementary analysis supports the robustness of the principal findings while also confirming the methodological value of deriving cortical labels through individual-level surface-based registration.

Results

Geodesic distances and connection distances

The GDs between the 180 cortical regions in the left hemisphere are shown in Fig. 2, the corresponding CDs in Fig. 3, and the corresponding Numbers of Streamlines in Fig. 4. The maximum SN between a pair of cortical regions was 1.8×10^5, and is shown in Fig. 4 clipped at 100 for the threshold and limited at 2,000 to provide a useful view of the numbers.

Downloaded from academic.oup.com/cercor/article/36/10/bhag176/9002283 by guest on 27 October 2026

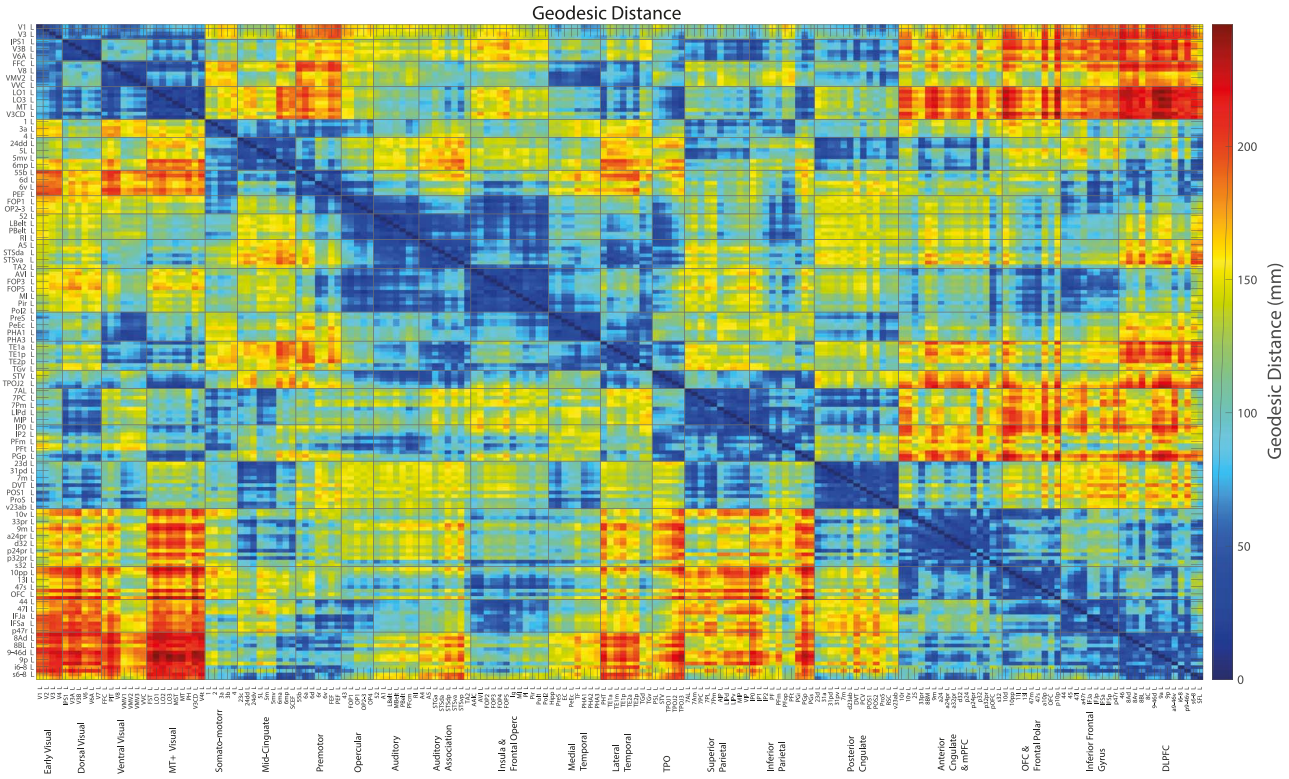


Figure 2 GD between HCP-MMP cortical regions in mm. The different cortical divisions are indicated by black lines with labels below. The abbreviations for the cortical regions, and the names of the cortical divisions, are shown in Table S1. Alternate labels are shown on the vertical axis for clarity in this and similar figures. Views of the human brain to show the sulci are shown in Fig. S1.

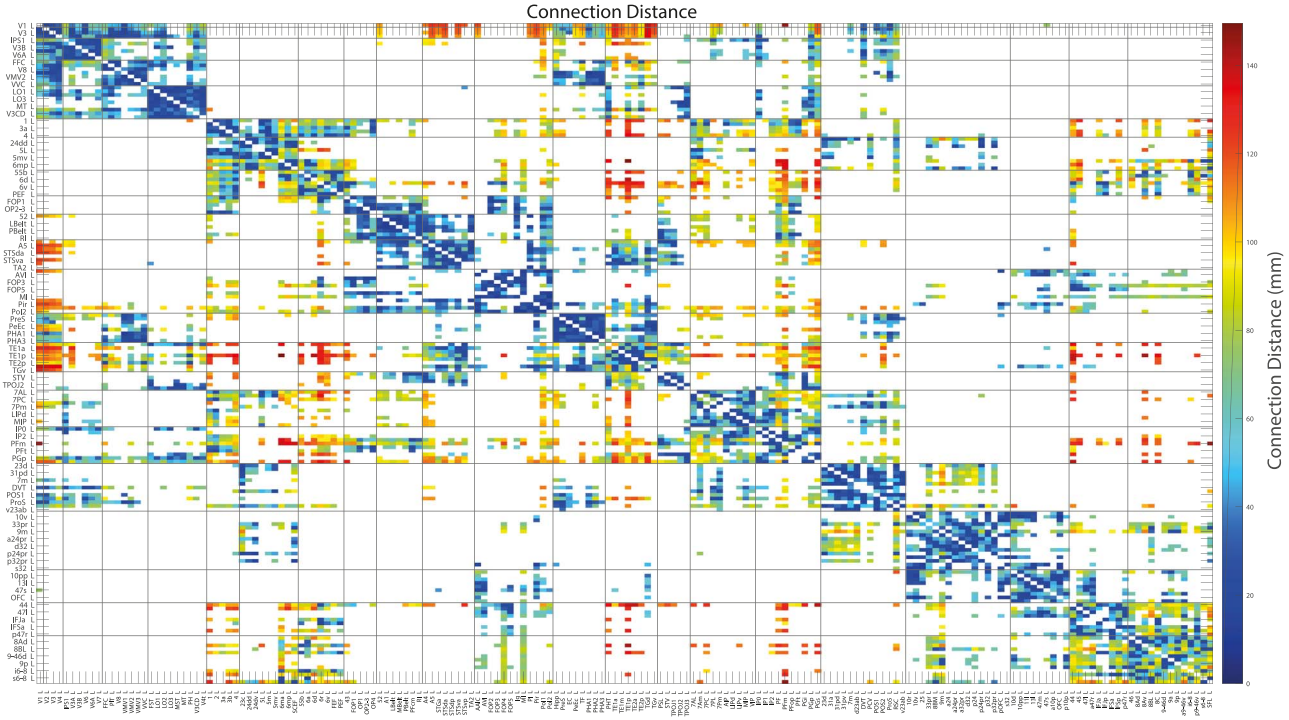


Figure 3 CD between HCP-MMP cortical regions in mm. The different cortical divisions are indicated by black lines. Blank entries indicate no connection measured by whether the streamline count was above a noise/low threshold of 100. Note that the CD range is shorter than the geodesic CD range, but that each uses a color map for the complete range for each color map.

Downloaded from academic.oup.com/cercor/article/36/10/bhag176/9002283 by guest on 27 October 2026

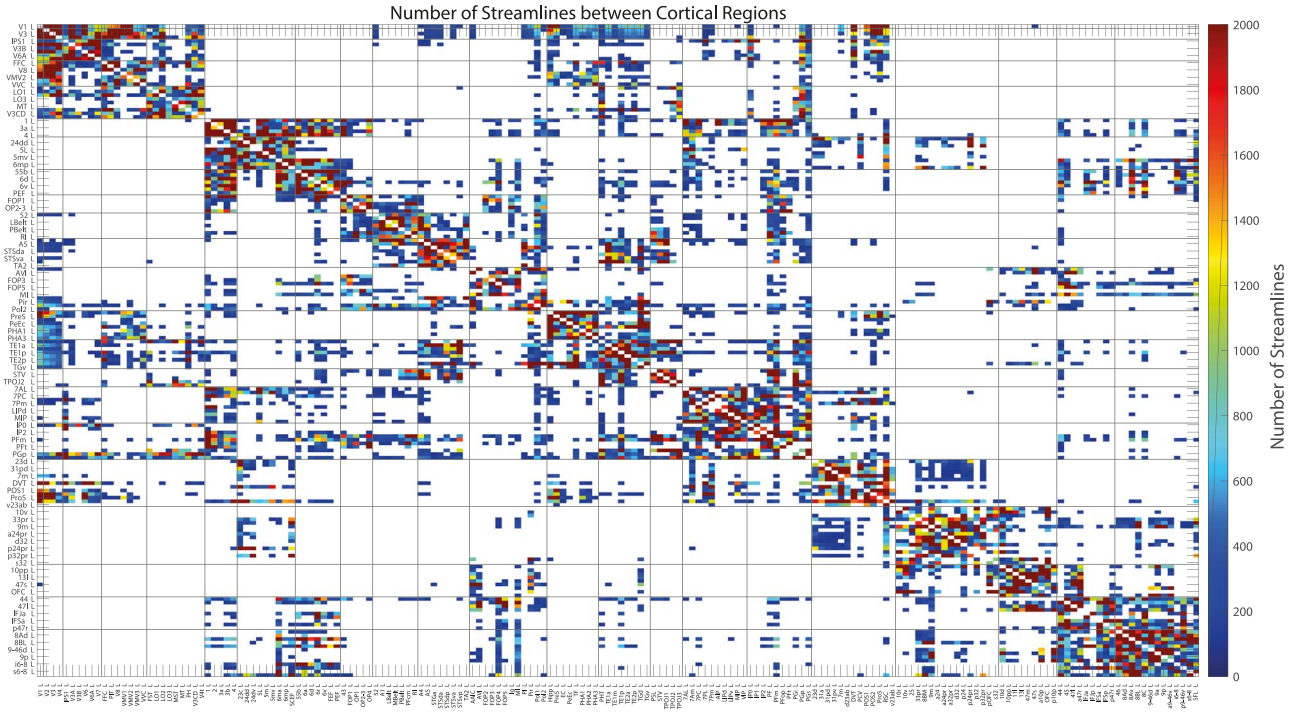


Figure 4 SN between HCP-MMP cortical regions. The different cortical divisions are indicated by black lines. Blank entries indicate no connection measured by whether the streamline count was above a noise/low threshold of 100. The maximum SN shown in the figure was clipped at 2,000, in order to show some of the differences for other cortical connections.

Link cost saving

The link cost saving is shown in Fig. 5. The link cost saving was measured by weighting the difference between the GD and the actual CD (in mm) multiplied by the SN in that connection. For the reasons stated in the Methods, cost savings are only considered for GDs ≥90 mm. Link cost savings in Fig. 5 are indicated by positive values. A number of examples of how these cost savings arise are provided in Table 1 and in Figs. 6–8 which show the paths of the streamlines, as described below. Negative values in Fig. 5 are relatively few, and indicate that for a few connections, the CD was longer than the GD. One example is the connection between area 44, part of Broca's area, and auditory cortex A4 in the temporal lobe for which the GD was 96 mm and the CD was 113 mm, as this connection is via the arcuate fasciculus.

Figure 5 and Tables 1 and S2 show that 1 cortical region with many cost savings for its direct connections is the Mid Insula (MI), which has high cost savings with some premotor cortical regions (eg 6ma, 6mp, 6a, 6d). For example, for the connections between region MI and region 6ma the direct streamline path length is 87 mm with the streamlines shown in Fig. 6b, the GD is 141 mm, and the link cost saving is 41,428 (Table 1). Understanding how this relates to sulci can be considered by comparison with the locations of these cortical regions in the folded brain in coronal slices (Fig. S1), which shows at $y = +10$ how the MI deep in the Sylvian fissure brings it much closer by a direct connection to premotor regions and to the somewhat more anterior dorsolateral prefrontal cortex regions, with this illustrated in Fig. 6b. In particular, Fig. 6b shows how the direct path is much shorter than would be connections across the surface of the unfolded cortex. Consistent with this, insular cortex regions such as MI have high link cost savings with a number of dorsolateral prefrontal cortex regions (eg 8BM, 8BL, 8Av, 8Ad, 9a, 9p, s6-8, and SFL). In addition, frontal opercular region 4 (FOP4) is close to MI, has similar connections, and benefits similarly from its location deep in the Sylvian fissure. This is an example of link cost savings that arise because at least 1 of the cortical regions is deep in a sulcus, in this case, regions FOP4 and MI. Part of the reason for the high link cost savings is that there are many streamlines between these insular and premotor cortex regions, consistent with the fact that the insular cortex regions are somatosensory cortical regions, which have high connectivity to premotor cortical regions that drive actions guided by somatosensory inputs (Rolls et al. 2023a; Rolls 2026a).

Another example of how connections between cortical regions can have high cost savings because at least 1 of the pair is in a sulcus is provided by PoI1 and PoI2 (posterior insula regions), which have high cost savings with parietal cortex regions including 7AL, 7PC, LIPv, MIP, PGp, PGs (Fig. 5 and Table S2; and Fig. S1 which shows that these posterior insular regions (at $y = -06$) benefit by being deep in the Sylvian fissure).

Just for comparison, regions that are close to each other on the cortical sheet have few cost savings, with for example the connections between region MI and region FOP4 having a direct streamline path length of 20 mm, and a GD of 25 mm (Fig. 6c).

For the connections between region 44 (part of Broca's area) and region 6ma, the direct streamline path length is 95 mm, the GD is 107 mm, and the link cost saving is 22,829 (Table 1). Figure 6a shows how although both of these regions are on gyri, the direct path followed by the streamlines is shorter than the geodesic path across the surface map, because of an intervening sulcus. Thus, the cortical folding in this type of case allows two cortical regions on gyri to bypass the long distance that would be needed across the surface map if there was no intervening sulcus, and to provide high link cost savings.

Downloaded from academic.oup.com/cercor/article/36/10/bhag176/9002283 by guest on 27 October 2026

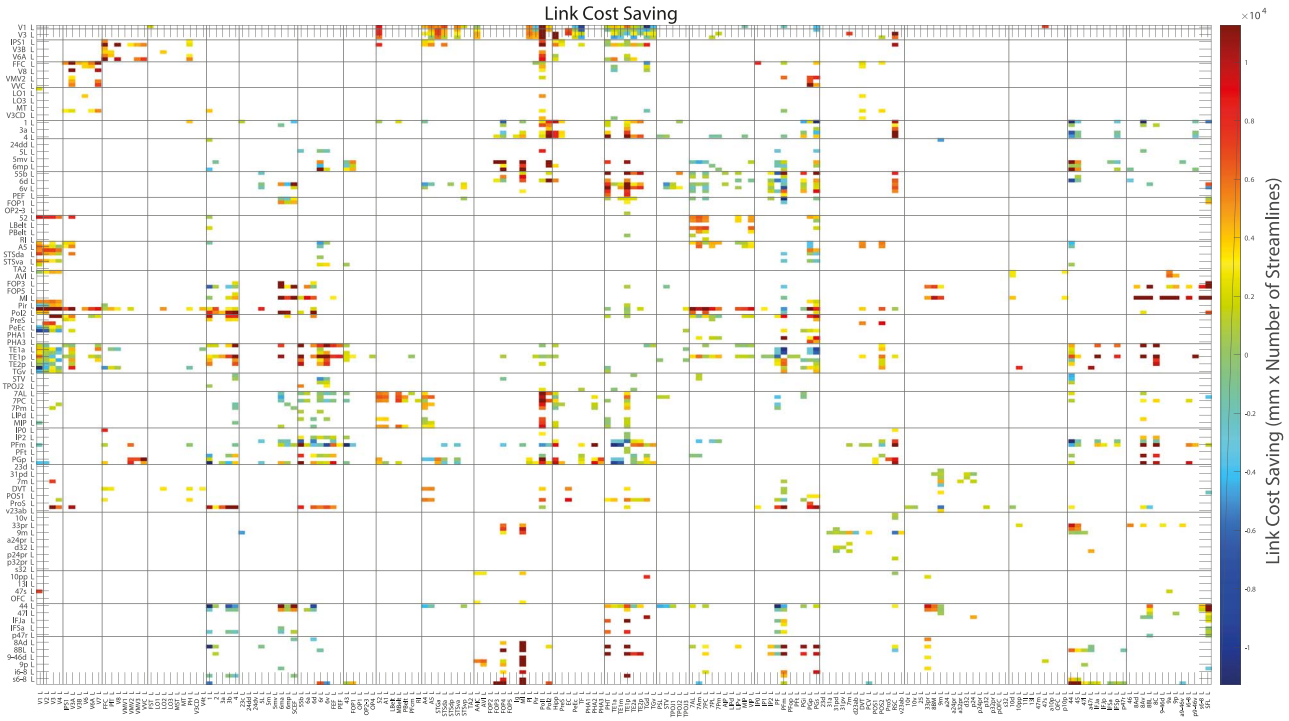


Figure 5 Link cost savings for HCP-MMP cortical regions in the left hemisphere. The different cortical divisions are indicated by black lines. Blank entries indicate connections that were not plotted because the GD was <90 mm, the streamline count was <100, or no connection was measured. The link cost saving was calculated by weighting the difference between the GD and the actual CD (in mm) multiplied by the SN in that connection. The minimum value of the GD considered was ≥90 mm, and links with fewer than 100 streamlines were excluded to ensure that low random values which in any case would not be associated with large savings did not contribute to what is shown.

Table 1 For selected pairs of cortical regions illustrated in Figs 6–8, the SN, GD, and direct CD, and the length cost savings calculated as the number of mm saved by a direct connection compared to a GD × the SN. The units of the cost savings are SN × distance in mm. The CostSavings are calculated from the exact values not the rounded values shown in the rest of the table. (Streamline# - Streamline Number, SN; GD - Geodesic Distance; CD - Connection Distance)

Region1	Region2	Streamline#	GD	CD	CostSavings
44	6ma	1,903	107	95	22,829
MI	6ma	769	141	87	41,428
MI	FOP4	5,584	25	20	26,156
PHT	8C	382	180	125	20,927
TE1p	6v	781	153	126	21,078
TE1p	8C	619	184	134	30,832
PGp	Hipp	235	137	103	7,950
PFm	PHA2	212	146	89	12,222

Another way in which sulci can influence the cost savings is if the cortical regions are not in sulci but are on gyri, but can benefit by not having to traverse the whole surface distance of the cortex that is in the sulcus. Examples are provided by the connections between temporal cortical visual regions such as PHT and TE1p and premotor regions such as 6d, 6r, and 55b. The direct path is shorter, as illustrated by the streamlines between TE1p and 8C, as illustrated in Fig. 7c and Table 1, which show link cost savings of 30,832 for a direct path length of 134 mm compared to a GD across the unfolded cortical map of 184 mm. This path is shorter than having to follow the surface route across the intervening insula. Further similar examples are PHT with 8C (Fig. 7a and Table 1), and TE1p with 6v (Fig. 7b and Table 1).

Further examples of cost savings involve the connectivity of the hippocampal memory system (Rolls 2023b, 2025, 2026a, 2026c). For example, for the connections between the Hippocampus (Hipp) and inferior parietal cortex region PGp, the direct CD is 103 mm, the GD is 137 mm, and the link cost saving is 7,950 (Table 1), with the actual streamline path shown in Fig. 8a. In another example, for the connections between the medial parahippocampal cortex region PHA2 (Huang et al. 2021; Rolls et al. 2022) and the inferior parietal visual region PFm (Rolls et al. 2023b), the direct CD is 89 mm, the GD is 146 mm, and the link cost saving is 12,222 (Table 1), with the actual streamline path shown in Fig. 8b. The streamlines in Fig. 8b illustrate well how the direct path of the streamlines is much shorter than the GD.

To enable the cost savings analysis to be systematic, the cost savings for every pair of connected cortical areas were ranked, with the first 100 links in the ranking shown in Table S2. Many examples are evident in Table S2 of how high link cost savings for particular connections are related to the sulci shown in Fig. S1, including the

Downloaded from academic.oup.com/cercor/article/36/10/bhag176/9002283 by guest on 27 October 2026

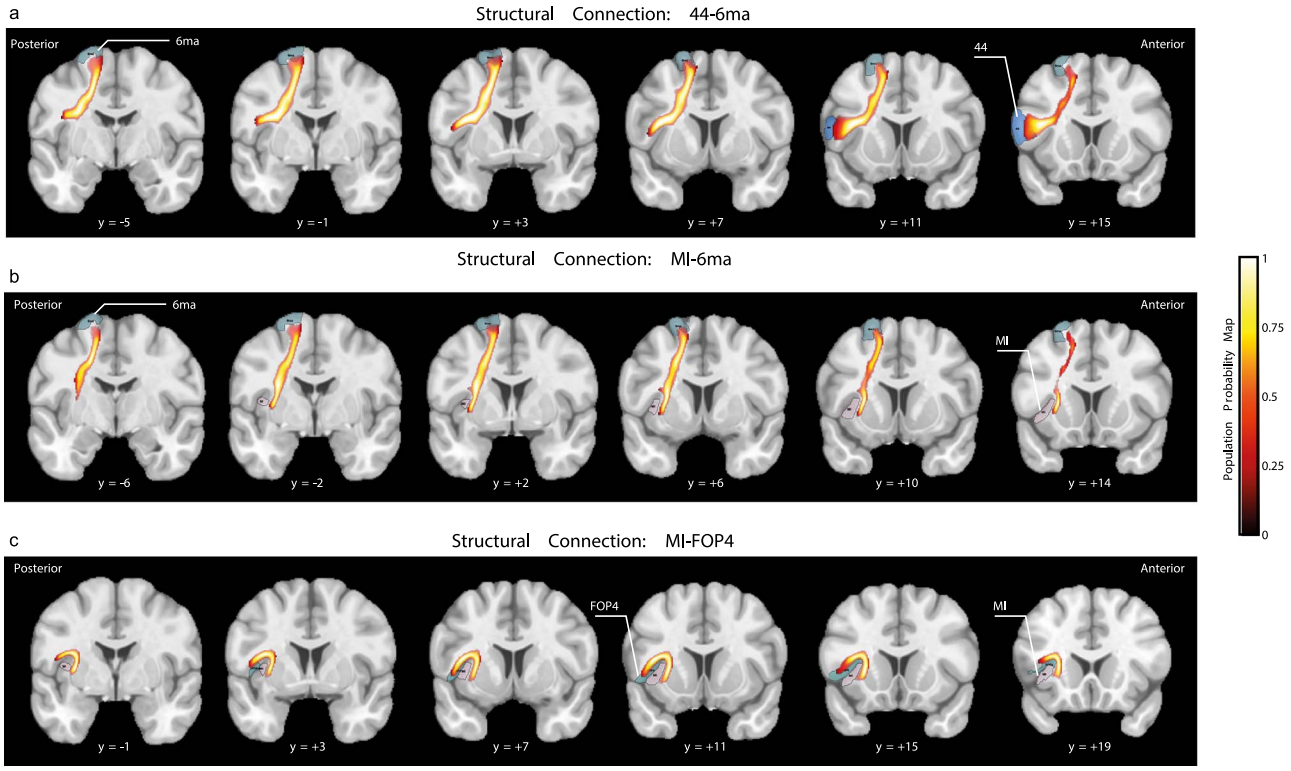


Figure 6 Examples of the streamline paths for some of the connections to illustrate how the direct path followed by some connections is shorter than the geodesic path along the cortical surface. a) For the connections between region 44 and region 6ma the direct streamline path length is 95 mm, and the GD is 107 mm. In the slice at $y = +10$, the single dashed red line shows what is meant by the GD, and how it can be longer than the actual CD of the streamlines between these cortical regions. The direct streamline path is longer than it looks in these slices, for it runs from $y = -5$ to $y = +15$. b) For the connections between region MI and region 6ma the direct streamline path length is 87 mm, and the GD is 141 mm. c) For the connections between region MI and region FOP4 the direct streamline path length is 20 mm, and the GD is 25 mm.

examples just presented. Similar findings were found to apply to the right hemisphere.

Discussion

In the research described here, we have shown that the direct CD for the streamline paths between some pairs of human cortical regions can be much shorter than the GD that would be required if the cortex was an unfolded surface. We have shown quantitatively how, using streamline diagrams (Figs. 6–8), this can arise if one or both cortical regions are in sulci. We have also shown how this can arise if both cortical regions are on gyri, but are separated by a sulcus (Figs. 6–8). We have also shown how a great deal of white matter can be saved, by weighting the CD saved for a pair of cortical regions as a result of the direct CD compared to the GD by the SN, to produce a weighted cost saving (Tables 1 and S2).

These quantitative analyses lead us to the following hypothesis about reasons that may contribute to why cortical folding occurs where it does. The hypothesis is that where certain pairs of cortical regions need to be connected by many connections to transfer information, the cortex will tend to fold to bring those cortical regions close together. The actual places where the folding occurs will be where, given the 180 × 180 matrix of connections (the number for the HCP-MMP atlas) between cortical regions, the folding will optimally minimize the total length of the white matter connections between all cortical regions. The length of white matter connections is estimated for any pair of cortical regions by the direct CD × the SN, and the folding helps to reduce that number compared to the GD in the unfolded cortex. That is proposed to be one factor in why cortical folding occurs where it does. There could be other reasons that might result in non-optimal folding, for example if a low direct CD is important because it minimizes conduction time in a system that must operate fast such as the dorsal visual system (Rolls 2024, 2026a). Another example might be that regions that develop and connect together early in embryological development might be weighted higher in the final folding solution.

An overall aim of cortical folding may be to minimize brain size and weight by reducing the total amount of white matter, which depends on the distance between each pair of cortical regions, and the number of connections between each pair of cortical regions (Rolls 2023a, 2026a). Keeping brain size low is important for many reasons, including in childbirth, and to minimize brain and head weight for land animals, which becomes especially important for humans that stand up and locomote (Rolls 2023a, 2026a).

The actual mechanisms by which the number of connections between pairs of cortical regions could be taken into account would include the tension-based models (Van Essen 1997; Van Essen et al. 2019; Van Essen 2020, 2023), in which having many connections between a pair of brain regions might lead to higher tension between those cortical regions, which could influence where the cortical folding occurs.

While our "Link Cost Saving" metric successfully quantifies the geometric advantages of sulci, specific limitations in methodology and interpretation can be considered. First, LinkCostSaving, defined

Downloaded from academic.oup.com/cercor/article/36/10/bhag176/9002283 by guest on 27 October 2026

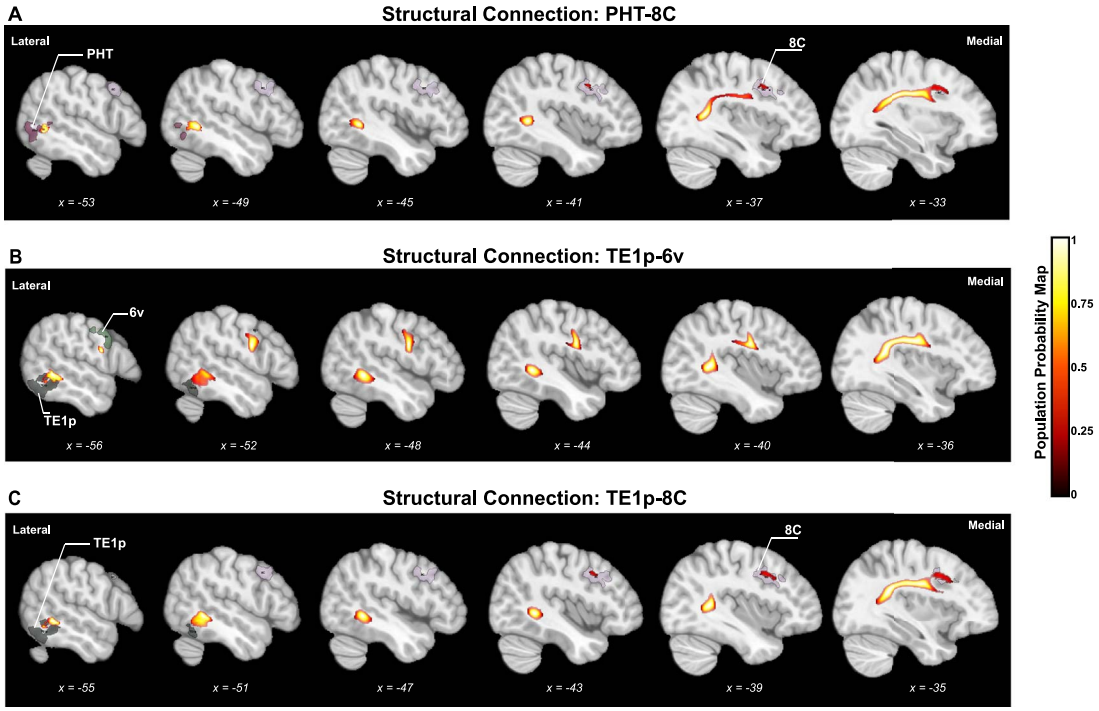


Figure 7 Examples of the streamline paths for some of the connections to illustrate how the direct path followed by some connections is shorter than the geodesic path along the cortical surface. For the connections between region PHT and region 8C the direct streamline path length is 125 mm, and the GD is 180 mm. For the connections between regionTE1p and region 6v the direct streamline path length is 126 mm, and the GD is 153 mm. For the connections between region TE1p and region 8C the direct streamline path length is 134 mm, and the GD is 184 mm.

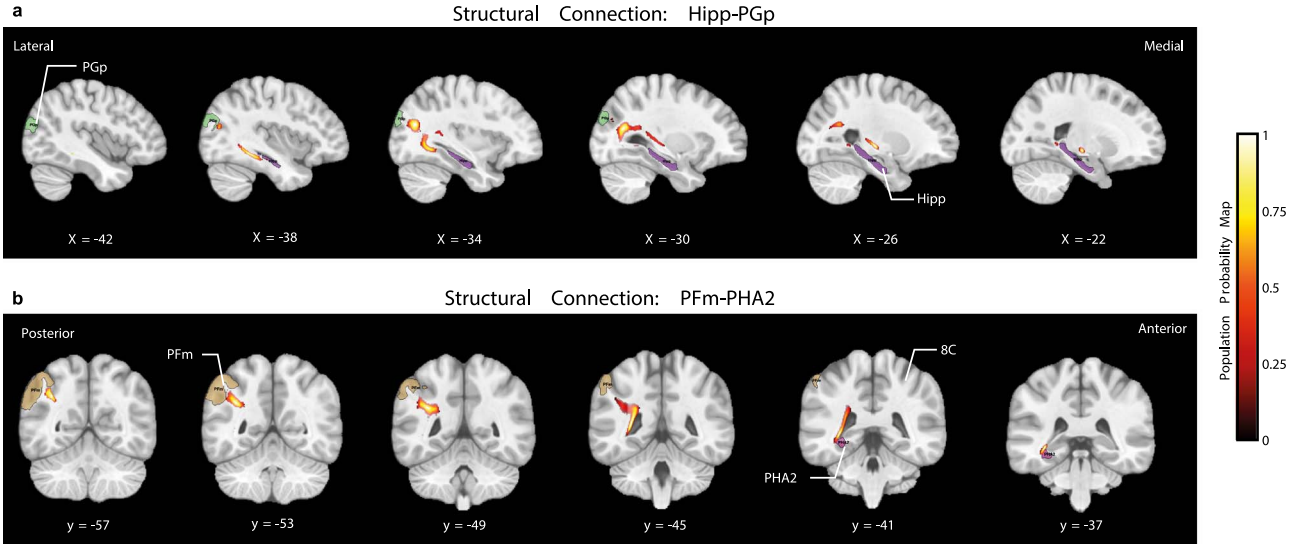


Figure 8 Examples of the streamline paths for some of the connections to illustrate how the direct path followed by some connections is shorter than the geodesic path along the cortical surface. For the connections between regions PGp and Hipp the direct streamline path length is 103 mm, and the GD is 137 mm. For the connections between regions PFm and PHA2 the direct streamline path length is 89 mm, and the GD is 146 mm.

as distance difference multiplied by streamline number that serves as a proxy for the amount of white matter needed to connect cortical regions, and therefore to influence total brain size, can be considered. It is not a direct measure of physical volume (or for that matter metabolic cost). Streamline counts derived from dMRI reflect probabilistic connectivity and microstructural integrity rather than absolute axon counts. Therefore, high-cost savings should be interpreted as a weighted optimization index of path geometry and connectivity confidence, rather than a precise biological measurement. However, and reassuringly, the correlation between the tractography-derived weighted streamline numbers and the tracer-derived connection numbers was 0.59 in the macaque cortex (Donahue et al. 2016), indicating that streamline numbers are a useful measure. Second, while the axonal tension hypothesis predicts that strong connections pull regions together to form gyri, our results show that non-adjacent strong connections (eg insula-premotor) gain efficiency by bridging sulci. This suggests that for long-range connections, sulcal formation represents a "compromise solution" under geometric constraints:

Downloaded from academic.oup.com/cercor/article/36/10/bhag176/9002283 by guest on 27 October 2026

minimizing wiring length while accommodating cortical expansion (Van Essen 1997; Van Essen et al. 2019; Van Essen 2020, 2023). Finally, our 90 mm threshold for the GDs excluded short-range U-fibers, which are the drivers of tension-based local folding (Van Essen et al. 2019; Van Essen 2020). Consequently, our findings probably reflect how long-range connections exploit existing macro-scale folds to optimize global efficiency, rather than explaining how local folds are initiated by short-range tension. This implies that cortical folding patterns emerge from the interplay between local developmental tension and whole-brain wiring optimization.

A further potential limitation is that current diffusion tractography is susceptible to gyral-crown bias, whereby streamline endpoints are preferentially reconstructed at gyral crowns rather than at sulcal banks or fundi (Schilling et al. 2018). Although using the median streamline length and aggregating connections within relatively large cortical parcels may reduce the influence of local endpoint bias, they do not eliminate it (Cottaar et al. 2021). Consequently, both connection-strength and connection-distance estimates may retain residual sampling bias.

Previous models of cortical folding have not addressed the key issue of why the sulci are where they are in the human and primate cortex (Van Essen 1997; Herculano-Houzel et al. 2010; Xu et al. 2010; Bayly et al. 2014; Fernandez et al. 2016; Kroenke and Bayly 2018; Heuer et al. 2019; Llinares-Benadero and Borrell 2019; Van Essen et al. 2019; Van Essen 2020, 2023; Heuer et al. 2025). We have produced quantitative analyses in this article that help to analyze some of the factors that may be involved. It will be of interest in future research to build a model based on the link cost savings approach described here of how these savings working together with an advantage to minimizing the total cost of the connections could lead to the actual cortical folding found in the real brain, as illustrated in Fig. S1. We note that in terms of geometry, cortical folding can help to reduce CDs between two cortical regions if both are in sulci; and for a cortical region in a gyrus to another cortical region that is more than one gyrus away.

In conclusion, based on the quantitative measures of CDs and the SN between each cortical region in the human brain, we propose that the actual sulcal placements offer a fundamental principle that may help to explain the macroscale organization of cortical folding by helping to minimize the amount of white matter connections between cortical regions, thereby helping to minimize the size of the brain. Minimizing brain size is important for childbirth, and minimizing brain weight is important for locomotion especially in terrestrial bipedal species. We note that developmental factors may give rise to additional constraints. We also propose that another advantage of the actual cortical folding found is that it brings relatively close together the components of some key hierarchically organized cortical processing streams such as the visual cortical streams in order to minimize conduction time and therefore brain processing time and response times. This research advances our understanding of cortical folding by providing quantitative measures of GDs, tract CDs, numbers of streamlines for each connection, and an estimate of the amount of white matter saved by each direct connection in the cortex, for the human brain. This type of quantitative approach is essential for understanding better a key property of the cerebral cortex, its folding.

Acknowledgments

Use of data from the HCP is warmly acknowledged. The HCP, WU-Minn Consortium (Principal Investigators: David Van Essen and Kamil Ugurbil; 1U54MH091657) received funding by the 16 NIH Institutes and Centers that support the NIH Blueprint for Neuroscience Research; and by the McDonnell Center for Systems Neuroscience at Washington University. We also thank Professor Zheng Wang (Peking University) for his kind support to YH throughout this work. No generative AI tools were used in the writing of the article.

Author contributions

Edmund T. Rolls (Conceptualization, Data curation, Formal analysis, Investigation, Methodology, Project administration, Resources, Software, Supervision, Validation, Visualization, Writing—original draft, Writing—review & editing), Yichun Huang (Conceptualization, Data curation, Formal analysis, Investigation, Methodology, Software, Validation, Visualization, Writing—review & editing), and Chu-Chung Huang (Conceptualization, Data curation, Formal analysis, Funding acquisition, Investigation, Methodology, Resources, Software, Validation, Visualization, Writing—review & editing)

Supplementary material

Supplementary material is available at *Cerebral Cortex* online.

Funding

This work was supported by Ministry of Science and Technology of the People's Republic of China (MOST, China, https://most.gov.cn/index.html) grant STI2030—Major Projects (2022ZD0213400) to C-CH. The funders had no role in study design, data collection and analysis, decision to publish, or preparation of the manuscript.

Conflicts of interest

The authors have no competing interests to declare.

Data and code availability

The data for the diffusion tractography described here was downloaded from the HCP (http://www.humanconnectome.org/). Data were provided [in part] by the HCP, WU-Minn Consortium (Principal Investigators: David Van Essen and Kamil Ugurbil; 1U54MH091657) funded by the 16 NIH Institutes and Centers that support the NIH Blueprint for Neuroscience Research; and by the McDonnell Center for Systems Neuroscience at Washington University.

The code for the diffusion tractography analysis described here is available as Supplementary Material in CorticalFoldingCode.zip.

Some of the articles and books referred to here are available for download from the website of the Oxford Center for Computational Neuroscience, https://www.oxcns.org.

Ethical permissions

No data were collected as part of the research described here. The data were from the HCP, and the WU-Minn HCP Consortium obtained full informed consent from all participants; and research procedures and ethical guide-lines were followed in accordance with the Institutional Review Boards, with details at the HCP website (http://www.humanconnectome.org/).

Downloaded from academic.oup.com/cercor/article/36/10/bhag176/9002283 by guest on 27 October 2026

References

Bayly PV, Taber LA, Kroenke CD. 2014. Mechanical forces in cerebral cortical folding: a review of measurements and models. *J Mech Behav Biomed Mater*. 29:568–581. https://doi.org/10.1016/j.jmbbm.2013.02.018.

Burt JB, Helmer M, Shinn M, Anticevic A, Murray JD. 2020. Generative modeling of brain maps with spatial autocorrelation. *Neuroimage*. 220:117038. https://doi.org/10.1016/j.neuroimage.2020.117038.

Cottaar M et al. 2021. Modelling white matter in gyral blades as a continuous vector field. *Neuroimage*. 227:117693. https://doi.org/10.1016/j.neuroimage.2020.117693.

Donahue CJ et al. 2016. Using diffusion tractography to predict cortical connection strength and distance: a quantitative comparison with tracers in the monkey. *J Neurosci*. 36:6758–6770. https://doi.org/10.1523/JNEUROSCI.0493-16.2016.

Fernandez V, Borrell V. 2023. Developmental mechanisms of gyrification. *Curr Opin Neurobiol*. 80:102711. https://doi.org/10.1016/j.conb.2023.102711.

Fernandez V, Llinares-Benadero C, Borrell V. 2016. Cerebral cortex expansion and folding: what have we learned? *EMBO J*. 35:1021–1044. https://doi.org/10.15252/embj.201593701.

Glasser MF et al. 2013. The minimal preprocessing pipelines for the human connectome project. *Neuroimage*. 80:105–124. https://doi.org/10.1016/j.neuroimage.2013.04.127.

Glasser MF et al. 2016. A multi-modal parcellation of human cerebral cortex. *Nature*. 536:171–178. https://doi.org/10.1038/nature18933.

Herculano-Houzel S, Mota B, Wong P, Kaas JH. 2010. Connectivity-driven white matter scaling and folding in primate cerebral cortex. *Proc Natl Acad Sci U S A*. 107:19008–19013. https://doi.org/10.1073/pnas.1012590107.

Heuer K et al. 2019. Evolution of neocortical folding: a phylogenetic comparative analysis of MRI from 34 primate species. *Cortex*. 118:275–291. https://doi.org/10.1016/j.cortex.2019.04.011.

Heuer K et al. 2025. *Principles of neocortical organisation and behaviour in primates*. bioRxiv:2025.2007. 2017.665410.

Huang C-C, Rolls ET, Hsu C-CH, Feng J, Lin C-P. 2021. Extensive cortical connectivity of the human hippocampal memory system: beyond the "what" and "where" dual-stream model. *Cereb Cortex*. 31:4652–4669. https://doi.org/10.1093/cercor/bhab113.

Huang CC, Rolls ET, Feng J, Lin CP. 2022. An extended human connectome project multimodal parcellation atlas of the human cortex and subcortical areas. *Brain Struct Funct*. 227:763–778. https://doi.org/10.1007/s00429-021-02421-6.

Kroenke CD, Bayly PV. 2018. How forces fold the cerebral cortex. *J Neurosci*. 38:767–775. https://doi.org/10.1523/JNEUROSCI.1105-17.2017.

Llinares-Benadero C, Borrell V. 2019. Deconstructing cortical folding: genetic, cellular and mechanical determinants. *Nat Rev Neurosci*. 20:161–176. https://doi.org/10.1038/s41583-018-0112-2.

Lv Y et al. 2023. Cerebral cortical regions always connect with each other via the shortest paths. *Cereb Cortex*. 33:9212–9222. https://doi.org/10.1093/cercor/bhad197.

Rolls ET. 2016. *Cerebral cortex: principles of operation*. Oxford University Press. https://doi.org/10.1093/acprof:oso/9780198784852.001.0001.

Rolls ET. 2023a. *Brain computations and connectivity*. Oxford University Press, Open Access. https://doi.org/10.1093/oso/9780198887911.001.0001.

Rolls ET. 2023b. Hippocampal spatial view cells for memory and navigation, and their underlying connectivity in humans. *Hippocampus*. 33:533–572. https://doi.org/10.1002/hipo.23467.

Rolls ET. 2024. Two what, two where, visual cortical streams in humans. *Neurosci Biobehav Rev*. 160:105650. https://doi.org/10.1016/j.neubiorev.2024.105650.

Rolls ET. 2025. Hippocampal discoveries: spatial view cells, connectivity, and computations for memory and navigation, in primates including humans. *Hippocampus*. 35:e23666. https://doi.org/10.1002/hipo.23666.

Rolls ET. 2026a. *Brain computations and principles; and AI*. Oxford University Press, Open Access.

Rolls ET. 2026b. *Neuroscience discoveries*. MIT Press, Open Access. https://doi.org/10.7551/mitpress/18504.001.0001.

Rolls ET. 2026c. Hippocampal revolutions. *Neurosci Biobehav Rev*. 180:106492. https://doi.org/10.1016/j.neubiorev.2025.106492.

Rolls ET, Deco G, Huang CC, Feng J. 2022. The effective connectivity of the human hippocampal memory system. *Cereb Cortex*. 32:3706–3725. https://doi.org/10.1093/cercor/bhab442.

Rolls ET, Deco G, Huang CC, Feng J. 2023a. Prefrontal and somatosensory-motor cortex effective connectivity in humans. *Cereb Cortex*. 33:4939–4963. https://doi.org/10.1093/cercor/bhac391.

Rolls ET, Deco G, Huang CC, Feng J. 2023b. The human posterior parietal cortex: effective connectome, and its relation to function. *Cereb Cortex*. 33:3142–3170. https://doi.org/10.1093/cercor/bhac266.

Schilling K et al. 2018. Confirmation of a gyral bias in diffusion MRI fiber tractography. *Hum Brain Mapp*. 39:1449–1466. https://doi.org/10.1002/hbm.23936.

Smith RE, Tournier JD, Calamante F, Connelly A. 2012. Anatomically-constrained tractography: improved diffusion MRI streamlines tractography through effective use of anatomical information. *Neuroimage*. 62:1924–1938. https://doi.org/10.1016/j.neuroimage.2012.06.005.

Smith RE, Tournier JD, Calamante F, Connelly A. 2013. SIFT: spherical-deconvolution informed filtering of tractograms. *Neuroimage*. 67:298–312. https://doi.org/10.1016/j.neuroimage.2012.11.049.

Smith RE, Tournier JD, Calamante F, Connelly A. 2015a. SIFT2: enabling dense quantitative assessment of brain white matter connectivity using streamlines tractography. *Neuroimage*. 119:338–351. https://doi.org/10.1016/j.neuroimage.2015.06.092.

Smith RE, Tournier JD, Calamante F, Connelly A. 2015b. The effects of SIFT on the reproducibility and biological accuracy of the structural connectome. *Neuroimage*. 104:253–265. https://doi.org/10.1016/j.neuroimage.2014.10.004.

Tournier J-D, Calamante F, Connelly A. 2010. Improved probabilistic streamlines tractography by 2nd order integration over fibre orientation distributions. *Proc Intl Soc Mag Reson Med (ISMRM)*. 18:1670.

Van Essen DC. 1997. A tension-based theory of morphogenesis and compact wiring in the central nervous system. *Nature*. 385:313–318. https://doi.org/10.1038/385313a0.

Van Essen DC. 2020. A 2020 view of tension-based cortical morphogenesis. *Proc Natl Acad Sci U S A*. 117:32868–32879. https://doi.org/10.1073/pnas.2016830117.

Van Essen DC. 2023. Biomechanical models and mechanisms of cellular morphogenesis and cerebral cortical expansion and folding. *Semin Cell Dev Biol*. 140:90–104. https://doi.org/10.1016/j.semcdb.2022.06.007.

Van Essen DC et al. 2019. Cerebral cortical folding, parcellation, and connectivity in humans, nonhuman primates, and mice. *Proc Natl Acad Sci U S A*. 116:26173–26180. https://doi.org/10.1073/pnas.1902299116.

Xu G et al. 2010. Axons pull on the brain, but tension does not drive cortical folding. *J Biomech Eng*. 132:071013. https://doi.org/10.1115/1.4001683.

Yu Y, Cai Q, Lin L, Huang CC. 2025. Fiber length distribution characterizes the brain network maturation during early school-age. *Neuroimage*. 308:121066. https://doi.org/10.1016/j.neuroimage.2025.121066.

© The Author(s) 2026. Published by Oxford University Press. All rights reserved. For commercial re-use, please contact reprints@oup.com for reprints and translation rights for reprints. All other permissions can be obtained through our RightsLink service via the Permissions link on the article page on our site—for further information please contact journals.permissions@oup.com.
Cerebral Cortex, 2026, **36**, bhag176
https://doi.org/10.1093/cercor/bhag176
Original Article

Downloaded from academic.oup.com/cercor/article/36/10/bhag176/9002283 by guest on 27 October 2026